Water Splitting Hot Paper

Deutsche Ausgabe: DOI: 10.1002/ange.201604091
Internationale Ausgabe: DOI: 10.1002/anie.201604091

Spatially Separated Photosystem II and a Silicon Photoelectrochemical Cell for Overall Water Splitting: A Natural–Artificial Photosynthetic Hybrid

Wangyin Wang[+], Hong Wang[+], Qingjun Zhu, Wei Qin, Guangye Han, Jian-Ren Shen, Xu Zong, and Can Li**

Abstract: *Integrating natural and artificial photosynthetic platforms is an important approach to developing solar-driven hybrid systems with exceptional function over the individual components. A natural–artificial photosynthetic hybrid platform is formed by wiring photosystem II (PSII) and a platinum-decorated silicon photoelectrochemical (PEC) cell in a tandem manner based on a photocatalytic-PEC Z-scheme design. Although the individual components cannot achieve overall water splitting, the hybrid platform demonstrated the capability of unassisted solar-driven overall water splitting. Moreover, H_2 and O_2 evolution can be separated in this system, which is ascribed to the functionality afforded by the unconventional Z-scheme design. Furthermore, the tandem configuration and the spatial separation between PSII and artificial components provide more opportunities to develop efficient natural–artificial hybrid photosynthesis systems.*

Producing hydrogen via photocatalytic or photoelectrochemical (PEC) water splitting is an attractive pathway for the conversion solar energy into chemical energy.[1] One of the half-reactions of water splitting, the oxygen evolution reaction (OER), is regarded as a major bottleneck owing to the high activation energy for O–O bond formation and the slow, four-electron reaction dynamics involved in artificial photosynthesis.[2] However, in natural photosynthesis, Photosystem II (PSII), the only water oxidation enzyme in nature, can capture light with wavelengths up to ca. 680 nm and accomplish OER at a low overpotential under mild conditions.[3] Moreover, as PSII can be separated from photosynthetic organisms, it could be an ideal platform for investigating the conversion and storage of solar energy.[4] Actually, exploiting photosynthetic proteins as a new class of photovoltaic materials for solar energy conversion has been under intense investigation.[5] Among these efforts, research on establishing natural–artificial hybrid system received much interest owing to its potential of integrating the merits of both the natural and artificial photosynthetic systems.[6] In a recent proof-of-concept study, we constructed a prototype natural–artificial hybrid system based on PSII and inorganic photocatalyst for unassisted solar water splitting.[7] In this system, PSII acts as an OER center and inorganic photocatalyst works as the hydrogen evolution reaction (HER) center, and these two components were integrated via redox couples based upon a traditional Z-scheme configuration. This work paves the way for the integration of natural and artificial systems for solar H_2 production from water splitting.

However, we note that the as-established natural–artificial hybrid system bears some intrinsic limitations. First, similar with the traditional Z-scheme system composed of two powdered photocatalysts, H_2 and O_2 will be readily mixed (Supporting Information, Scheme S1).[8] This will lead to undesirable back-reaction between O_2 and H_2 and bring potential safety issues. Second, PSII and photocatalyst powder are intimately mixed. If these two components can be spatially separated but kept connected in some way, there will be more opportunities to flexibly optimize the individual components in the hybrid system without considering their complex and unidentified interactions. Finally, PSII can capture light with wavelengths up to ca. 680 nm and exhibit good performance for OER.[9] On the contrary, most semiconductor materials generally require irradiation at short wavelengths, and are inefficient for OER under irradiation at long wavelengths.[1c] Constructing a tandem system that allows complementary solar absorption by semiconductor materials (short wavelength irradiation) and PSII (long wavelength irradiation) will enable better utilization of incident light for solar fuel production.[10] To tackle these issues, it is highly desirable to establish a viable route to bridge the natural and artificial photosynthetic systems.

Herein, we constructed a photocatalytic-PEC Z-scheme system by integrating a traditional powder-based Z-scheme

[*] Dr. W. Y. Wang,[+] H. Wang,[+] Dr. W. Qin, Prof. Dr. X. Zong, Prof. Dr. C. Li
State Key Laboratory of Catalysis, Dalian Institute of Chemical Physics, Chinese Academy of Sciences, Dalian National Laboratory for Clean Energy, The Collaborative Innovation Center of Chemistry for Energy Materials (iChEM)
Zhongshan Road 457, Dalian, 116023 (China)
E-mail: xzong@dicp.ac.cn
canli@dicp.ac.cn
H. Wang,[+] Q. J. Zhu
University of Chinese Academy of Sciences
Beijing 100049 (China)
Q. J. Zhu, Dr. G. Y. Han, Prof. Dr. J. Shen
Photosynthesis Research Center, Key Laboratory of Photobiology, Institute of Botany, Chinese Academy of Sciences
Beijing 100093 (China)
Prof. Dr. J. Shen
Photosynthesis Research Center, Graduate School of Natural Science and Technology, Okayama University
1-1, Naka 3-chome, Tsushima, Okayama 700-8530 (Japan)
[+] These authors contributed equally to this work.

Supporting information for this article can be found under: http://dx.doi.org/10.1002/anie.201604091.

photocatalytic system and film-based PEC system with the aid of mediators. According to this Z-scheme design, a novel natural–artificial hybrid platform with a tandem configuration was constructed by wiring photosystem II and a platinum-decorated silicon photoelectrochemical cell. The hybrid platform is capable of achieving unassisted solar water splitting with spatially separated H_2 and O_2 evolution. Moreover, the tandem design and the spatial isolation between natural and artificial components provide more opportunities to develop efficient natural–artificial hybrid systems.

The configuration of the prototype natural–artificial hybrid platform is shown in Scheme 1. The platform is a combination of a traditional Z-scheme photocatalytic system and a two-compartment PEC system. One compartment contains PSII for photocatalytic O_2 evolution and the other contains a PEC cell for PEC H_2 evolution. The two compartments are separated with a Nafion film but are connected by a wire with the aid of redox species such as $[Fe(CN)_6]^{3-}/[Fe(CN)_6]^{4-}$.

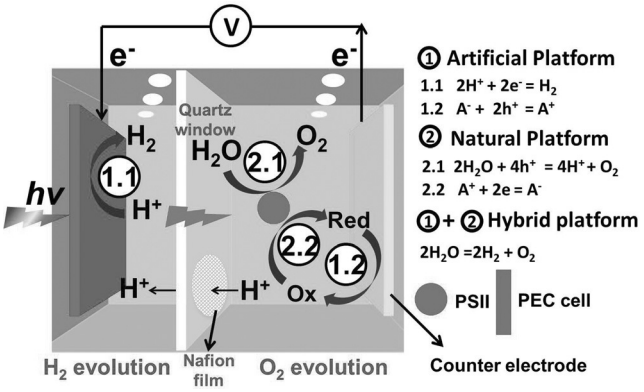

Scheme 1. Illustration of the natural–artificial platform with a tandem configuration based on photocatalytic-PEC Z-scheme design.

In the cathodic compartment, PEC cell absorbs light at short wavelengths and produces H_2 using photogenerated electrons (reaction 1.1). In the meantime, photogenerated holes will transport to the counter electrode and oxidize $[Fe(CN)_6]^{4-}$ to $[Fe(CN)_6]^{3-}$ in the anodic compartment (reaction 1.2). Due to the rectification of the junction formed between PEC cell and electrolyte interface,[1b] photogenerated charges will be separated spontaneously, which will remediate the undesirable back-reaction between redox species and PEC cell.

In the anodic compartment, PSII absorbs the irradiation passing through the photocathode and catalyzes water oxidation to produce O_2 (reaction 2.1). At the same time, $[Fe(CN)_6]^{3-}$ produced in the PEC reaction is restored to $[Fe(CN)_6]^{4-}$ by the electrons from PSII (reaction 2.2).

Therefore, PEC H_2 evolution on the artificial platform and photocatalytic O_2 evolution on the natural platform can be integrated into a reaction cycle with the aid of the redox couple. From this point, a photocatalytic-PEC Z-scheme loop that integrates the merits of both photocatalytic and PEC systems is established. This system is capable of achieving unassisted solar water splitting. Moreover, the Nafion membrane sandwiched between the two compartments allows for the separation of H_2 and O_2 produced, which is more advantageous than the traditional Z-scheme design. Furthermore, the tandem design of the platform allows the absorption of short wavelength light by the semiconductor and long wavelength light by PSII, which enables efficient utilization of solar energy.

As a proof-of-concept study, we initially investigated the individual processes that could occur in the hybrid platform (for experimental details, see the Supporting Information). These studies are expected to provide useful information for the subsequent integration studies. PSII core complexes were isolated from the thermophilic cyanobacterium *T. vulcanus* as described previously.[11] The oxygen evolution capacity achieved with this PSII can reach up to 3580 μmol O_2 (mg of Chl)$^{-1}$ h^{-1} under optimum conditions (Supporting Information, Figure S1). We first investigated the oxygen evolution performance of PSII in the presence of $[Fe(CN)_6]^{3-}$ as the electron acceptor by a Clark-type oxygen electrode under saturated red light irradiation. No O_2 was evolved when PSII was absent in the electrolyte (Figure 1 A). With the addition of 2.5 μg Chl $mL^{-1}$of PSII, O_2 was evolved at a rate of 24.9 μmol h^{-1} and the rate of oxygen evolution increased linearly with the amount of PSII (Figure 1 B). Photocatalytic O_2 evolution reactions were also conducted for a longer duration, and similar results were obtained (Supporting Information, Figure S2).

We then investigated the enzymatic kinetics dependence of PSII on the concentration of $[Fe(CN)_6]^{3-}$. O_2 evolution was not observed when $[Fe(CN)_6]^{3-}$ was absent in the electrolyte (Figure 1 C). With the addition of a 1 mM of $[Fe(CN)_6]^{3-}$ as the electron acceptor, O_2 evolution with an impressive rate of 14.8 μmol h^{-1} was obtained. Further increase in the amount of

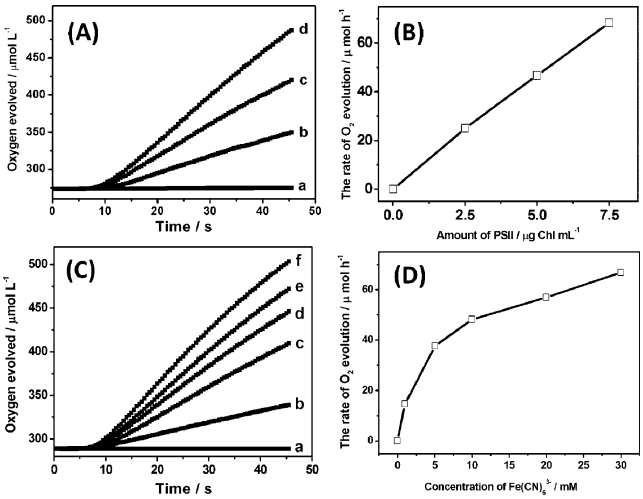

Figure 1. A) Time courses of photocatalytic O_2 evolution using a) 0, b) 2.5, c) 5, and d) 7.5 μg Chl mL^{-1} PSII in the presence of 10 mM $[Fe(CN)_6]^{3-}$ as electron acceptors. B) The initial rate of O_2 evolution with the amount of PSII used. C) Time courses of photocatalytic O_2 evolution using a) 0, b) 1, c) 5, d) 10, e) 20, and f) 30 mM $[Fe(CN)_6]^{3-}$ as electron acceptor in the presence of 6 μg Chl mL^{-1} PSII. D) The initial rate of O_2 evolution with the amount of $[Fe(CN)_6]^{3-}$ used. Light source: saturated red light ($\lambda > 600$ nm). The amount of O_2 evolved is measured using a Clark-type oxygen electrode.

$[Fe(CN)_6]^{3-}$ to 10 and 30 mM led to substantial increase in the rate of O_2 evolution (Figure 1D). The relationship between the initial rate of oxygen evolution and the concentration of $[Fe(CN)_6]^{3-}$ indicates that the photocatalytic reaction follows Michaelis–Menten kinetics (Supporting Information, Figure S3).[12]

After achieving photocatalytic O_2 evolution on PSII, we aimed to achieve PEC H_2 evolution on PEC cell. Transparent double-junction Si solar cells were prepared with chemical vapor deposition and covered with an indium-doped tin oxide (ITO) top layer and Pt catalyst as the HER catalyst. The cell exhibited a short-circuit photocurrent density of 3.1 mA cm^{-2}, an open-circuit voltage of 1.2 V, and incident photon-to-current conversion efficiency (IPCE) of lower than 40% under whole solar spectrum (Supporting Information, Figure S4). We note that the performance of the Si solar cell is not good. However, as it can provide sufficient voltage to drive the oxidation of $[Fe(CN)_6]^{4-}$ to $[Fe(CN)_6]^{3-}$ (standard redox potential of 0.71 V vs. RHE), it could be used to demonstrate the design in this proof-of-concept study.

The PEC properties of the platinum-decorated Si solar cell were investigated by operation of the cell as a photocathode in a two-electrode configuration at zero applied bias. The influence of the concentration of $[Fe(CN)_6]^{4-}$ on the rate of H_2 evolution obtained on the platinum-decorated Si PEC cell was first investigated. No appreciable photocurrent was observed when $[Fe(CN)_6]^{4-}$ was absent in the anodic compartment (Supporting Information, Figure S5). When only 5 mM of $[Fe(CN)_6]^{4-}$ was used in the anodic compartment, an appreciable photocurrent density of ca. 0.53 mA cm^{-2} was obtained (Supporting Information, Figure S5). As the redox potential of $[Fe(CN)_6]^{4-}/[Fe(CN)_6]^{3-}$ is ca. 0.71 V vs. RHE more negative than that of O_2/H_2O, the addition of $[Fe(CN)_6]^{4-}$ can release the stringent requirement on the oxidation part of the overall reaction and therefore enables the H_2 evolution reaction in the cathodic compartment. When the concentration of $[Fe(CN)_6]^{4-}$ was further increased to 10, 15, and 20 mM, the photocurrent density was concurrently increased to 0.73, 0.8, and 0.88 mA cm^{-2}, respectively. Therefore, increasing the $[Fe(CN)_6]^{4-}$ concentration in the anodic compartment is beneficial for enhancing the HER in the cathodic compartment.

The amount of H_2 evolved in the cathodic compartment and $[Fe(CN)_6]^{3-}$ produced in the anodic compartment were analyzed by gas chromatography and UV/Vis absorption spectroscopy. We found that H_2 can be produced with an average rate of 33 μmol h^{-1} at a Faradic efficiency of about 90% after 2 hours of reaction in the cathodic compartment (Figure 2A,B). Moreover, we observed the steady generation of $[Fe(CN)_6]^{3-}$ with an Faradic efficiency of ca. 100% in the anodic compartment (Figure 2C,D). Therefore, the observed photocurrent during Chronoamperometry test was mainly related with the H_2 evolution reaction in the cathodic compartment and the $[Fe(CN)_6]^{4-}$ oxidation reaction in the anodic compartment, and the H_2 evolution on platinum-decorated Si PEC cell can be realized by using $[Fe(CN)_6]^{4-}$ as electron donor.

After establishing a photocatalytic system that can achieve O_2 evolution with natural PSII and a PEC system

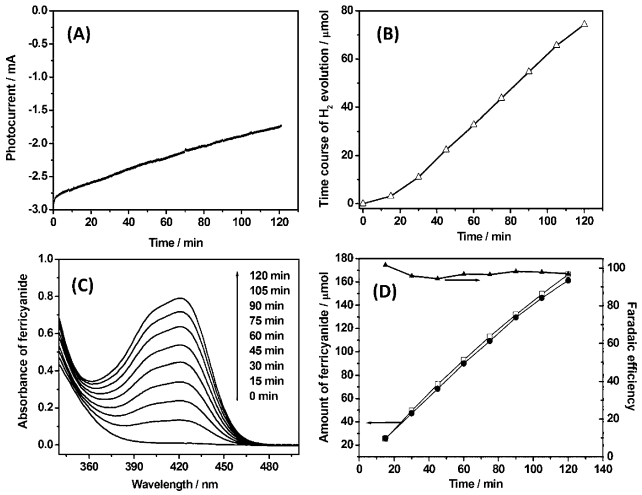

Figure 2. A) Chronoamperometry curve obtained on platinum-decorated Si PEC cell in a two-electrode system at zero bias under visible irradiation, electrode area: 4 cm^{-2}; B) the corresponding time course of H_2 evolution in the cathodic compartment; C) UV/Vis absorption spectra of the solution in the anodic compartment, which indicates the gradual generation of $[Fe(CN)_6]^{3-}$; and D) the Faradaic efficiency for $[Fe(CN)_6]^{3-}$ production. The concentration of $[Fe(CN)_6]^{4-}$ is 20 mM. Light source: 300 W Xe lamp (250 mW cm^{-2}) with a cutoff filter of 420 nm.

that can achieve autonomous H_2 evolution on a platinum-decorated Si PEC cell, respectively, we sought to construct a fully light-driven hybrid bioinorganic system for overall water splitting reaction. In this step, we wired the two components according to the configuration shown in Scheme 1 using the $[Fe(CN)_6]^{4-}/[Fe(CN)_6]^{3-}$ redox couples as a bridge.

As we aimed to establish a tandem system that allows the absorption of solar irradiation at short wavelengths by artificial component and that at long wavelengths by PSII in sequence, we first checked whether PSII remains active for O_2 evolution in this tandem configuration. UV/Vis absorption analysis shows that the Si PEC cell absorbs most irradiation at short wavelengths, allowing the transmission of irradiation with $\lambda > 650$ nm that can excite PSII (Figure 3A). Photocatalytic reactions indicated that O_2 can be evolved at a rate of 16 μmol h^{-1} on PSII when using the Si PEC cell as the light filter (Figure 3B). This is similar with the result obtained when using the 600 nm light filter. Therefore, there PSII can retain good OER performance in the present tandem configuration.

We then performed overall water splitting reaction in the hybrid system. In a typical experiment, $[Fe(CN)_6]^{4-}$ was used in the anodic compartment. In this case, the water splitting reaction is initiated from the H_2 evolution reaction instead of the O_2 evolution reaction. Figure 3C shows typical time courses of H_2 and O_2 evolution in the cathodic and anodic compartment of hybrid system, respectively. It was found that H_2 was produced at a rate of 30 μmol h^{-1} in the cathodic compartment and O_2 was evolved at a rate of 15 μmol h^{-1} in the anodic compartment. The TOF of water oxidation by PSII is calculated to be 1.4 s^{-1} in the first hour, which is comparable with that of the PSII-based devices previously reported.[5c]

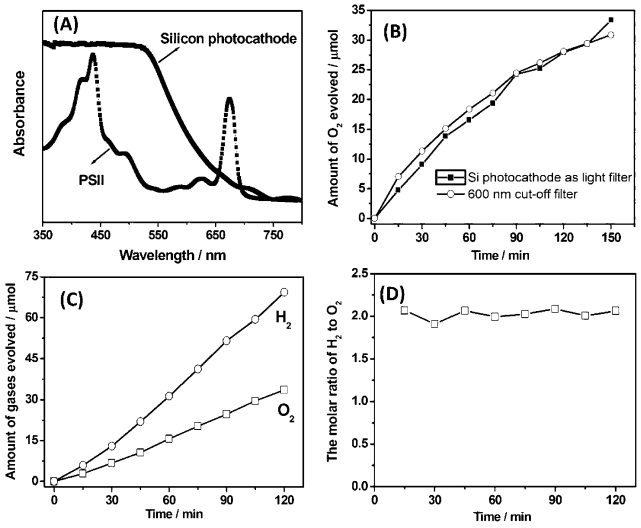

Figure 3. A) UV/Vis absorption spectra of the platinum-decorated Si PEC cell and PSII. B) Time courses of photocatalytic O_2 evolution using Si photocathode or a cutoff filter ($\lambda > 600$ nm) as light filter. C) Time courses of O_2 and H_2 evolution from overall water splitting in the tandem system. D) Molar ratio of as-produced H_2 to O_2 during the reaction. 5 μg Chl mL^{-1} PSII and 10 mM $[Fe(CN)_6]^{4-}$ were used during the reaction. Light source: 300 W Xe lamp (250 mW cm^{-2}) with a cutoff filter of 420 nm.

The molar ratio of H_2 to O_2 gases is calculated to be about 2, which provides strong evidence that overall water splitting was successfully achieved in the hybrid platform (Figure 3D). The solar-to-hydrogen efficiency is calculated to be about 0.29% when measured under standard solar irradiation (AM 1.5G, 100 mW cm^{-2}; Supporting Information, Figure S6). Moreover, as H_2 and O_2 were evolved in the cathodic and anodic compartments, respectively, the gas separation issue existing in the traditional Z-scheme system can be resolved. Therefore, we clearly demonstrated that the natural and artificial components in the hybrid system can be spatially separated while connected to achieve a circuit for unassisted solar water splitting with separated H_2 and O_2 evolution.

During the reaction, $[Fe(CN)_6]^{3-}$ will be produced as an intermediate in the anodic compartment. The simultaneous generation of the stoichiometric amount of H_2 and O_2 indicates that PSII can consume the $[Fe(CN)_6]^{3-}$ intermediate and produce O_2 with a high efficiency. This is further supported by the negligible change in the color of the reaction solution in the anodic compartment during the reaction (Supporting Information, Figure S7). In sharp contrast, when we performed the reaction in the absence of PSII, the solution in the anodic compartment turned to deep yellow due to the accumulation of yellow $[Fe(CN)_6]^{3-}$ (Supporting Information, Figure S8).

We also attempted to start the overall water splitting reaction from the water oxidation reaction. In this case, most reaction parameters were the same except for replacing $[Fe(CN)_6]^{4-}$ with $[Fe(CN)_6]^{3-}$. Typical time courses of H_2 and O_2 evolution in the cathodic and anodic compartment, respectively, are shown in the Supporting Information, Figure S9. We found that O_2 can be produced at an average rate of 30 μmol h^{-1} in the anodic compartment. However, H_2 is produced with much lower rate than O_2. This indicates that the $[Fe(CN)_6]^{4-}$ intermediate produced in the anodic compartment cannot be consumed efficiently by the Si PEC cell to produce equivalent amount of H_2. Therefore, although the as-produced O_2 and H_2 are actually from water splitting, the rate of H_2 evolution does not match with that of O_2 evolution and the rate-determining step of the overall water splitting reaction is supposed to be the H_2 evolution reaction. However, considering the results shown in Figure 3, if we speculate that the Si PEC cell and PSII are stable enough, the rate of H_2 and O_2 evolution will finally reach balance with the increase of $[Fe(CN)_6]^{4-}$ and the decrease of $[Fe(CN)_6]^{3-}$ during prolonged reaction.

The results obtained in the present study have several important implications. First, we showed that natural and artificial photosynthetic systems can be bridged based on a photocatalytic–PEC Z-scheme strategy and achieve unassisted solar water splitting with separated H_2 and O_2 evolution. Second, the spatial isolation of the natural enzyme from the artificial system will allow for flexible optimization of the individual components in the hybrid system without considering their complex interaction. For example, although we demonstrated that the hybrid system can achieve autonomous overall water splitting at zero bias, we can also apply a small bias to the Si PEC cell to tune the rate of H_2 evolution (Supporting Information, Figure S10). Moreover, it is also possible to improve the efficiency of the system by optimizing the preparation of the Si PEC cell, changing the amount of PSII and the type of redox couples. For the present system, the water splitting performance is mainly limited by the Si PEC cell, and optimization of the Si solar cell is underway. Finally, the tandem design in the present study enables complementary light absorption by the two components in the hybrid system, which is beneficial for efficient utilization of solar irradiation.

In summary, we integrated PSII into the artificial circuit of a PEC cell using a photocatalytic-PEC Z-scheme strategy. The natural-artificial hydrid platform is capable of achieving unassisted solar water splitting with spatially separated H_2 and O_2 evolution using a pathway inaccessible in biology under solar irradiation. This proof-of-concept study is important because it affords an amenable route to bridge naturel and artificial systems, which allows them to harness the strengths inherent to both inorganic materials chemistry and biology for the efficient production of solar fuel. It is expected that a more efficient natural–artificial water-splitting platform will be established through integrating the ample gallery of photosynthesis enzymes and highly active PEC cells.

Acknowledgements

This work was financially supported by 973 National Basic Research Program of the Ministry of Science and Technology (Grant 2014CB239403), National Natural Science Foundation of China (No. 21090340), and the Key Research Program of the Chinese Academy of Science (No. KGZD-EW-T05). X.Z. acknowledges the financial support from Young Thousand Talents Program of China.

Keywords: photocatalysis · photoelectrochemistry · photosystem II · water splitting · Z-scheme

How to cite: *Angew. Chem. Int. Ed.* **2016**, *55*, 9229–9233
Angew. Chem. **2016**, *128*, 9375–9379

[1] a) A. J. Bard, M. A. Fox, *Acc. Chem. Res.* **1995**, *28*, 141–145; b) M. G. Walter, E. L. Warren, J. R. McKone, S. W. Boettcher, Q. X. Mi, E. A. Santori, N. S. Lewis, *Chem. Rev.* **2010**, *110*, 6446–6473; c) A. Kudo, Y. Miseki, *Chem. Soc. Rev.* **2009**, *38*, 253–278.

[2] a) M. W. Kanan, Y. Surendranath, D. G. Nocera, *Chem. Soc. Rev.* **2009**, *38*, 109–114; b) L. Duan, F. Bozoglian, S. Mandal, B. Stewart, T. Privalov, A. Llobet, L. Sun, *Nat. Chem.* **2012**, *4*, 418–423; c) D. Gust, T. A. Moore, A. L. Moore, *Acc. Chem. Res.* **2009**, *42*, 1890–1898.

[3] a) J. Barber, *Chem. Soc. Rev.* **2009**, *38*, 185–196; b) B. Loll, J. Kern, W. Saenger, A. Zouni, J. Biesiadka, *Nature* **2005**, *438*, 1040–1044; c) Y. Umena, K. Kawakami, J.-R. Shen, N. Kamiya, *Nature* **2011**, *473*, 55–60; d) H. Dau, I. Zaharieva, *Acc. Chem. Res.* **2009**, *42*, 1861–1870; e) J.-R. Shen, *Annu. Rev. Plant Biol.* **2015**, *66*, 23–48.

[4] R. E. Blankenship, D. M. Tiede, J. Barber, G. W. Brudvig, G. Fleming, M. Ghirardi, M. R. Gunner, W. Junge, D. M. Kramer, A. Melis, T. A. Moore, C. C. Moser, D. G. Nocera, A. J. Nozik, D. R. Ort, W. W. Parson, R. C. Prince, R. T. Sayre, *Science* **2011**, *332*, 805–809.

[5] a) S. K. Ravi, S. C. Tan, *Energy Environ. Sci.* **2015**, *8*, 2551–2573; b) O. Yehezkeli, R. Tel-Vered, J. Wasserman, A. Trifonov, D. Michaeli, R. Nechushtai, I. Willner, *Nat. Commun.* **2012**, *3*, 742; c) M. Kato, J. Z. Zhang, N. Paul, E. Reisner, *Chem. Soc. Rev.* **2014**, *43*, 6485–6497; d) O. Yehezkeli, R. Tel-Vered, D. Michaeli, I. Willner, R. Nechushtai, *Photosynth. Res.* **2014**, *120*, 71–85; e) G. Ulas, G. W. Brudvig, *J. Am. Chem. Soc.* **2011**, *133*, 13260–13263.

[6] a) P. Cai, X. Feng, J. Fei, G. Li, J. Li, J. Huang, J. Li, *Nanoscale* **2015**, *7*, 10908–10911; b) J. O. Calkins, Y. Umasankar, H. O'Neill, R. P. Ramasamy, *Energy Environ. Sci.* **2013**, *6*, 1891–1900; c) W. Wang, Z. Wang, Q. Zhu, G. Han, C. Ding, J. Chen, J.-R. Shen, C. Li, *Chem. Commun.* **2015**, *51*, 16952–16955.

[7] W. Wang, J. Chen, C. Li, W. Tian, *Nat. Commun.* **2014**, *5*, 4647.

[8] a) R. Abe, T. Takata, H. Sugihara, K. Domen, *Chem. Commun.* **2005**, 3829–3831; b) R. Abe, K. Sayama, K. Domen, H. Arakawa, *Chem. Phys. Lett.* **2001**, *344*, 339–344; c) M. Higashi, R. Abe, A. Ishikawa, T. Takata, B. Ohtani, K. Domen, *Chem. Lett.* **2008**, *37*, 138–139; d) M. Higashi, R. Abe, T. Takata, K. Domen, *Chem. Mater.* **2009**, *21*, 1543–1549; e) D. J. Martin, P. J. T. Reardon, S. J. A. Moniz, J. W. Tang, *J. Am. Chem. Soc.* **2014**, *136*, 12568–12571; f) S. Chen, Y. Qi, T. Hisatomi, Q. Ding, T. Asai, Z. Li, S. S. K. Ma, F. Zhang, K. Domen, C. Li, *Angew. Chem. Int. Ed.* **2015**, *54*, 8498–8501; *Angew. Chem.* **2015**, *127*, 8618–8621.

[9] D. Mersch, C.-Y. Lee, J. Z. Zhang, K. Brinkert, J. C. Fontecilla-Camps, A. W. Rutherford, E. Reisner, *J. Am. Chem. Soc.* **2015**, *137*, 8541–8549.

[10] J. H. Kim, H. Kaneko, T. Minegishi, J. Kubota, K. Domen, J. S. Lee, *ChemSusChem* **2016**, *9*, 61–66.

[11] a) J. R. Shen, Y. Inoue, *Biochemistry* **1993**, *32*, 1825–1832; b) J.-R. Shen, N. Kamiya, *Biochemistry* **2000**, *39*, 14739–14744.

[12] S. Khan, J. S. Sun, G. W. Brudvig, *J. Phys. Chem. B* **2015**, *119*, 7722–7728.

Received: April 27, 2016
Revised: May 30, 2016
Published online: June 27, 2016

